

where

$$F_m(v) = \frac{(-1)^m e^{iv} - e^{-iv}}{v^2 - (m\pi/2)^2}$$

and

$$\bar{I}_{m_p}^{lr} = \int_{-\infty}^{\infty} \frac{\zeta^2}{\kappa} F_m(\zeta a) F_p(-\zeta a) e^{i\zeta(l-r)T_a} d\zeta \quad (9)$$

Similarly, by using the boundary conditions at  $y = d$ , we obtain another simultaneous equation for  $\bar{c}_m^l$  and  $\bar{d}_m^l$ :

$$\frac{1}{\alpha\alpha} \sum_{m=0}^{\infty} \xi_m \bar{d}_m^l \left\{ \sum_{n=0}^{\infty} \frac{\bar{O}_{mn}^l \bar{O}_{pn}^r}{\gamma_n \tan(\gamma_n h)} \right\} = \varepsilon_p \bar{c}_p^r \quad (10)$$

where

$$\bar{O}_{mn}^l = \begin{cases} \frac{\alpha_n}{\alpha_n^2 - \alpha_m^2} \{ \sin[\alpha_n(a - \alpha - lT_a)] \\ + (-1)^m \sin[\alpha_n(a + \alpha + lT_a)] \} \\ 2a \end{cases} \quad \text{when } m = n = 0 \quad (11)$$

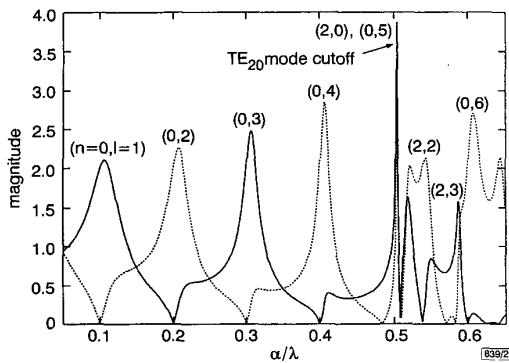


Fig. 2 Variation with frequency of magnitudes of fields at centre of rectangular cavity with single slot

$h = 5\alpha$ ,  $a = 0.01\alpha$ ,  $d = 0.02\alpha$ ,  $\theta = 0^\circ$   
 ———  $E_x$   
 .....  $H_z$

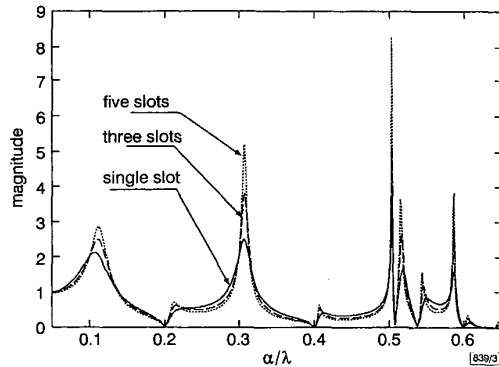


Fig. 3 Variation with frequency of magnitude of electric field at centre of multiple slotted rectangular cavity

$h = 5\alpha$ ,  $a = 0.01\alpha/N$  ( $N = 1, 3, 5$ : (number of slots)),  $d = 0.02\alpha$ ,  $T_a = 0.03\alpha$ ,  $\theta = 0^\circ$

**Numerical computations:** To illustrate the relation between the field formulation and the resonant modes,  $E_x^m$  at the centre inside the cavity from eqn. 5 is roughly given by

$$E_x^{III}(x = 0, y = d + h/2) \simeq \cos\left(\frac{n\pi}{2}\right) \sin\left(\gamma_n \frac{h}{2}\right) \quad (12)$$

and the  $E_x$ -field for the  $TE_n$  mode of the two-dimensional rectangular cavity without any slot is given by

$$E_x(\text{at the centre}) \simeq \cos\left(\frac{n\pi}{2}\right) \sin\left(\frac{l\pi}{2}\right) \quad (13)$$

Making the above equations equal, we can deduce the following relationship:

$$k_0^2 = \alpha_n^2 + \left(\frac{l\pi}{2}\right)^2 \quad (14)$$

Owing to the symmetry with respect to the  $y$ -axis, only even numbers are allowed for the index  $n$ . Fig. 2 shows the magnitudes of the electric and magnetic fields at the centre of the rectangular cavity with a single slot, where  $h = 5\alpha$ ,  $a = 0.01\alpha$ ,  $d = 0.02\alpha$ , for normal incidence ( $\theta = 0^\circ$ ). The resonant peaks come out slightly higher in frequencies than those corresponding to interior cavity modes as labelled in Fig. 2. The resonances of the electric and the magnetic fields occur in turn as the index  $l$  is increased. Note that the electric and magnetic fields are concurrently resonated at  $\alpha/\lambda = 0.5$ . This frequency is the cutoff frequency of the  $TE_{20}$  mode. And we also observe from Fig. 2 that the  $TE_{10}$  mode cannot be present inside the rectangular cavity because of the symmetry. The changes in resonance behaviours due to multiple slots are shown in Fig. 3. As the number of slots is increased, while keeping the total slot area the same, the resonant peaks are gradually sharpened. This means that the shielding property is improved as the number of slots is increased under constant total slot area.

**Conclusion:** Electromagnetic wave penetration into a two-dimensional multiple-slotted rectangular cavity with TE-wave has been investigated. By using the Fourier transform and the mode-matching technique, we have obtained a solution in a fast-converging series form. Numerical computations show the resonance and the penetration behaviours inside the cavity in terms of the size of the cavity and the slot and the number of slots.

© IEE 1999

16 November 1998

Electronics Letters Online No: 19990076

H.H. Park and H.J. Eom (Department of Electrical Engineering, Korea Advanced Institute of Science and Technology, 373-1, Kusong Dong, Yuseong Gu, Taejeon, Korea)

H.J. Eom is on sabbatical leave at the Department of Electronic and Electrical Engineering, The University of Sheffield, Sheffield S1 3JD, United Kingdom

## References

- 1 TEJEDOR, J.V., NUNO, L., and BATALLER, M.F.: 'Susceptibility analysis of arbitrarily shaped 2-D slotted screen using a hybrid generalized matrix finite-element technique', *IEEE Trans. Electromagn. Compat.*, 1998, **EMC-40**, (1), pp. 47-54
- 2 WANG, T.M., CUEVAS, A., and LING, H.: 'RCS of a partially open rectangular box in the resonant region', *IEEE Trans. Antennas Propagat.*, 1990, **AP-38**, (9), pp. 1498-1504
- 3 PARK, H.H., and EOM, H.J.: 'Electrostatic potential distribution through thick multiple rectangular apertures', *Electron. Lett.*, 1998, **34**, (15), pp. 1500-1501

## Encoding edge blocks by partial blocks of codevectors in vector quantisation

Hui-Hsun Huang, Cheng-Wen Ko and Chien-Ping Wu

A natural approach in vector quantisation to treat an edge block as two partial blocks and encode them with the partial blocks of the codevectors is proposed. This puts more bits on the edge blocks to improve their quality and only one codebook is used.

**Introduction:** Vector quantisation (VQ) is a widely used method for image compression. An important factor affecting the performance of VQ is the distortion of the edge blocks in the output image. These edge blocks dominate the others in the visual perception of the image, and so accurate encoding is highly desirable; however, because their contents are relatively complex, it is not easy to make a good approximation to them. In this Letter, we propose a natural approach to treat an edge block as two partial blocks and encode them with the partial blocks of the codevectors. This puts more bits on the edge blocks to improve their encoding. The same codebook is used for edge and non-edge blocks.

**Proposed encoding method:** Images are divided into non-overlapping blocks (4x4 in our experiment). A set of training vectors is used to make the codebook using the conventional LBG method [1] (with modifications, see below). This codebook will be used to encode all input blocks. At encoding, every block of the input image is classified as an 'edge' or 'non-edge' block at first. The nearest neighbour of a non-edge block in the codebook is found as its representative codevector and the index of this codevector is transmitted. For an edge block, we need three codewords to encode it. One is the type of its edge pattern, the other two are the indices of the representative vectors of the two parts of the block on each side of the edge, or its partial blocks. To find the representative vector of an input partial block, we choose the codevector whose corresponding partial block has the least distortion to the input. In other words, in the calculation of distance, only the pixels inside the range of the partial block are considered (see Fig. 1).

The decoder uses the same codebook and edge types as the encoder. The decoding is only a table looking procedure. For an edge block, the two representative codevectors are cut according to the edge type and put together to make the output block.

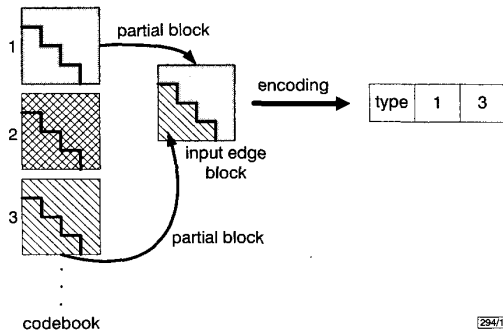


Fig. 1 Description of proposed method

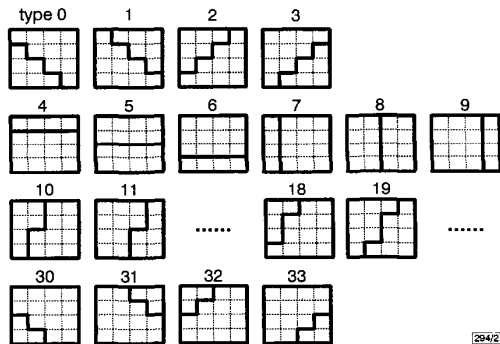


Fig. 2 Patterns of edge blocks

**Classification:** With the block size of 4x4, we group the edge blocks into 34 patterns with line edge segments (see Fig. 2). For an input block, the grey levels of the neighbouring pixels are compared. If the normalised difference between two neighbouring pixels exceeds a threshold, a gradient is considered to exist. We adopted the criteria of [2] and set the threshold as 0.2. If only gradients of the same direction exist in a certain row or column, then the one with the largest gradient is defined as the dominant gradient in that row or column. If there are gradients of both directions in the same row or column, then none is selected as the dominant gradient. Thus there is at most one dominant gradient on each row or column of pixels. For every input block, we count the number of its dominant gradients on the edges of various patterns. If at least three dominant gradients exist on the edges of a specific pattern (or four for type 0-3), the block is considered as belonging to that pattern. On a tie between two types, the type with the longer number or more continuous dominant gradients takes the block. If they still tie, arbitrary priority is assigned.

The classification only involves arithmetic and a finite number of comparisons and is only a small overhead compared with the codevector finding operations. By our criteria, an image typically

has about 10-15% of edge blocks. Because an edge block needs two more codewords than a non-edge block, this increases the total bit rate by 20-30%.

**Construction of the codebook:** In the codebook, the last 34 codewords are reserved to represent the 34 types of edge blocks, hence the 34 centroids with fewest average distortions in their clusters are not split during the last iteration of the LBG algorithm.



Fig. 3 Part of Lena image

a Original image  
 b Result of conventional VQ ( $M = 1024$ , 0.63 bit/pixel)  
 c Result of proposed method ( $M = 256$ , 0.62 bit/pixel)

Table 1: Comparison of results on 512x512 Lena image

	bit/pixel	Whole image		Edge blocks	
		MSE	PSNR	MSE	PSNR
Conventional VQ ( $M = 1024$ )	0.63	50.11	31.13	200.32	25.11
Proposed partial block method ( $M = 256$ )	0.62	51.29	31.03	136.94	26.76

$M$ : codebook size

**Simulation results:** We use eight 512x512 images with 8 bit/pixel as the training set. One image outside the training set, the 512x512 Lena image, is used as the test image. To have similar bit rates, a smaller size codebook ( $M = 256$ ) is used in our method to compare with a larger size codebook ( $M = 1024$ ) in the conventional method. The results are shown in Table 1 and Fig. 3. The bit rate and PSNR for the total image are similar in these two experiments, but our method outperforms the conventional methods on the edge blocks. This can be demonstrated by the PSNR calculated on only the edge blocks. Our method is 1.65dB better (see Table 1). Also note the edges on the parts of the output image in Fig. 3 (e.g. the shoulder, the border of the cheek and border of the hat).

**Discussion and perspectives:** Under the same bit rate, we distribute more bits to the edge blocks from the other part of the image to improve its quality. We consider the partial blocks as the truncated part of some non-edge blocks, thus the same codebook is used for all. The rationale of using the partial blocks of the codevectors is based on the assumption that the distortion is evenly distributed over all dimensions of the vectors. This is reasonable if the size of the training sets is not too small.

Our method, besides its easy design and coding by the single codebook, has another very important advantage. Because the partial blocks are similar to regular non-edge blocks, the interblock correlation of them with their neighbouring blocks will be much better than the whole edge block. Hence many concepts concerning the interblock correlations, such as predictive VQ, finite state VQ etc., can all be easily applied. By these improvements, the cost of edge blocks will be largely reduced and then larger codebooks and more detailed edge patterns can be used to achieve more efficient and accurate compression. In other words, we treat the partial blocks as a continuity of their neighbouring blocks. This makes our scheme conceptually very different from the other edge block methods such as block truncation coding

related VQ algorithm [3, 4]. Our method is a promising starting point for a very efficient image compression scheme.

**Conclusion:** We split an edge block in an image into two partial blocks and encode them with partial blocks of the vectors in the codebook. This natural approach improves the performance of VQ on the edges and also has good potential for further refinement.

© IEE 1999

13 November 1998

Electronics Letters Online No: 19990051

Hui-Hsun Huang, Cheng-Wen Ko and Chien-Ping Wu (Department of Electrical Engineering, National Taiwan University, Taipei, Taiwan, Republic of China)

Corresponding author: Chien-Ping Wu

## References

- 1 LINDE, Y., BUZO, A., and GRAY, R.M.: 'An algorithm for vector quantizer design', *IEEE Trans. Commun.*, 1980, **28**, (1), pp. 84-95
- 2 RAMAMURTHI, B., and GERSHO, A.: 'Classified vector quantization of images', *IEEE Trans. Commun.*, 1986, **34**, (11), pp. 1105-1115
- 3 MOHAMED, S.A., and FAHMY, M.M.: 'Image compression using VQ-BTC', *IEEE Trans. Commun.*, 1995, **43**, (7), pp. 2177-2182
- 4 WANG, C.C., CHEN, C.H., and CHEN, I.H.: 'Modified VQ-BTC algorithm for image compression', *Electron. Lett.*, 1998, **34**, (14), pp. 1390-1392

## Technique for accurate correspondence estimation in object borders and occluded image regions

E. Izquierdo M.

An advanced block-matching technique, in which the shape of the matching window is calculated adaptively by applying an energy-based model, is introduced. In this model the window shape is controlled by external forces defined according to the entropy of previously estimated disparities, their reliability and the variation of the image intensity.

**Introduction:** It is well-known that the correspondence problem is an inverse ill-posed optimisation problem where available information does not constrain the solution sufficiently and must therefore be regularised. Several techniques with different degrees of trade-off have been proposed to obtain an accurate solution. Pixel-correspondence estimation by hierarchical block-matching is a well-established technique in computer vision. Unfortunately, this approach can fail in sampling positions near to the borders of the objects. At these positions it is desirable to obtain good estimates, because the more accurate the displacement vectors calculated along the object contour are, the more reliable is the variation of the displacement field, and the more valuable is the information contained in these fields. To overcome this difficulty we propose to refine an initially estimated displacement field through an additional processing step, in which sampling positions with unreliable estimates are again matched, adapting the size and form of the reference window.

**Initial displacement estimation:** To obtain initial displacement fields, the hierarchical-block matching technique presented in [1] is applied. The reliability of the initial estimates is calculated using a criterion based on the uniqueness constraint [2, 3] together with the analysis of the curvature of the correlation surface generated during the initial hierarchical block-matching step [2]. Next, the initial disparity field is smoothed by applying a iterative filtering procedure, in which the degree of smoothing is weighted according to the reliability of the neighbouring vectors. In this schema each vector is updated using the average of the nearest neighbours weighted by their respective reliabilities.

**Matching with an adaptive window:** To improve the initial field, disparity vectors with low reliability values are estimated again. The goal is to choose a window size and shape that provides a new disparity estimate with higher reliability. To cope with this task we model the border of the matching window as an elastic contour  $\Omega$  with internal energy  $E_{int}$ . Starting with a sufficiently small contour  $\Omega_0$  around any sampling position  $z$ , it is deformed dynamically by external forces until a steady state is reached. Assuming that, near object borders, the available initial information has a high degree of uncertainty, whereas inside the objects the estimated disparities are more reliable, the external forces are defined according to the following three requirements: forces in the direction of sampling positions with reliable disparities should be large and they should be small in the direction of sampling positions with uncertain disparities (r1); the external force should tend to expand  $\Omega$  in the direction in which the disparity vectors show a smooth course while no expansion force should work in the direction of regions of the disparity field with high entropy (r2); and the external force should decrease continuously in proportion to the distance between  $z$  and  $\Omega$  (r3).

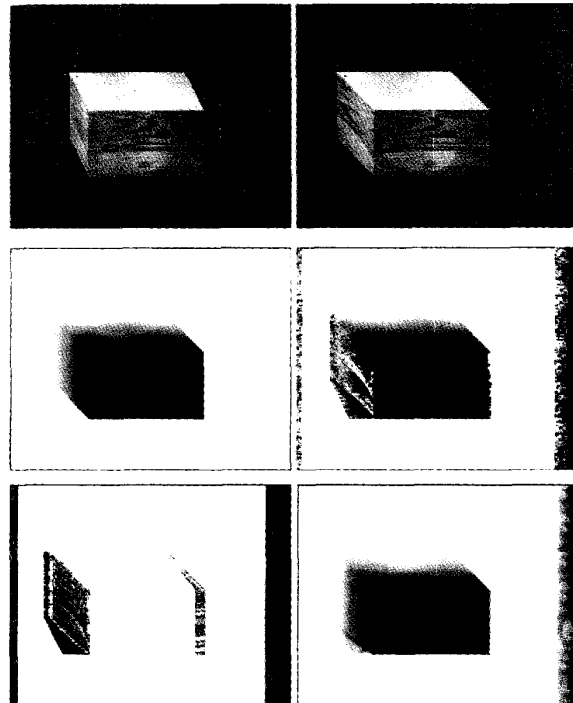


**Fig. 1** Stereoscopic scene with known exact disparity map (top), disparity map estimated by applying hierarchical block-matching approach (middle-right), corresponding reliability values (bottom-left) and disparity map by applying matching with adaptive window (bottom-right)

A general energy functional for the contour is  $E = \alpha E_{int} + \beta E_{ext}$ , where  $E_{int}$  represents the tension of the elastic contour (internal forces) and  $E_{ext} = \int_0^{2\pi} \int_0^{\rho(\theta)} F(\theta, \rho) d\rho d\theta$  is the energy produced by the external force  $F(\theta, \rho) = h_1(\tilde{z}, \sigma_\alpha^2) h_2(\tilde{z}, P_d)$  applied to each sampling position  $\tilde{z} = (\theta, \rho)$  (in polar co-ordinates) lying on  $\Omega$ , in the direction  $\theta$ .  $\sigma_\alpha^2$  measures the degree of smoothness of all disparity vectors in the region surrounded by  $\Omega$ ,  $h_1(\tilde{z}, \sigma_\alpha^2)$  is a function measuring the amount of support that  $\sigma_\alpha^2$  gives to  $F(\theta, \rho)$  and  $h_2(\tilde{z}, P_d)$  is a function measuring the amount of support that the reliability  $P_d$  of the disparity vector  $d$  in the position  $\tilde{z}$  gives to  $F(\theta, \rho)$ . Moreover, the functions  $h_1(\tilde{z}, \sigma_\alpha^2)$  and  $h_2(\tilde{z}, P_d)$  should be defined according to properties r1, r2 and r3.

A natural way to convert potential to kinetic energy is to expand iteratively the contour from its initial position until the potential becomes zero. To perform this process, we define a set of increasing contours  $\Omega_0 \subseteq \Omega_1 \subseteq \dots \subseteq \Omega_n$ . The potential in an intermediate step is given by  $E_{\Omega_i}^p = E_{\Omega_n} - E_{\Omega_i}$ , where  $E_{\Omega_n}^p = 0$ . The energy dissipation in each expansion step can be estimated as the decrement of the potential  $\Delta E_{\Omega_i}^p = |E_{\Omega_{i-1}}^p - E_{\Omega_i}^p|$ ,  $0 < i \leq n$ . Under the assumption that the external forces fulfil property r3, it is clear that  $E_{\Omega_n}^p = 0$ , if  $\Delta E_{\Omega_n}^p = 0$ . Consequently we can use the